J|A|C|S
ARTICLES

Published on Web 06/24/2009

Quantum Mechanical/Molecular Mechanical and Density Functional Theory Studies of a Prototypical Zinc Peptidase (Carboxypeptidase A) Suggest a General Acid−General Base Mechanism

Dingguo Xu*,† and Hua Guo*,‡

MOE Key Laboratory of Green Chemistry & Technology, College of Chemistry, Sichuan University, Chengdu, Sichuan 610064, P. R. China, and Department of Chemistry and Chemical Biology, University of New Mexico, Albuquerque, New Mexico 87131

Received April 7, 2009; E-mail: dgxu@scu.edu.cn; hguo@unm.edu

Abstract: Carboxypeptidase A is a zinc-containing enzyme that cleaves the C-terminal residue in a polypeptide substrate. Despite much experimental work, there is still a significant controversy concerning its catalytic mechanism. In this study, the carboxypeptidase A-catalyzed hydrolysis of the hippuryl-L-Phe molecule ($k_{cat} = 17.7 \pm 0.7\ s^{-1}$) is investigated using both density functional theory and a hybrid quantum mechanical/molecular mechanical approach. The enzymatic reaction was found to proceed via a promoted-water pathway with Glu270 serving as the general base and general acid. Free-energy calculations indicate that the first nucleophilic addition step is rate-limiting, with a barrier of 17.9 kcal/mol. Besides activating the zinc-bound water nucleophile, the zinc cofactor also serves as an electrophilic catalyst that stabilizes the substrate carbonyl oxygen during the formation of the tetrahedral intermediate. In the Michaelis complex, Arg127, rather than Zn(II), is responsible for the polarization of the substrate carbonyl and it also serves as the oxyanion hole. As a result, its mutation leads to a higher free-energy barrier, in agreement with experimental observations.

1. Introduction

Carboxypeptidase A (CPA), which contains a divalent zinc ion in its active site, is an important exopeptidase secreted by the pancreas for digesting intake proteins in the metabolism cycle. It catalyzes the elimination of the C-terminal amino acid via hydrolysis, with a preference toward residues with hydrophobic side chains.[1] Although peptides are the intended substrates, CPA can also hydrolyze other unnatural substrates, including esters. CPA is a representative member of the zinc hydrolase superfamily and has served as a prototype for understanding binding and catalysis of such enzymes.[2,3] As a result, the corresponding enzymatic reactions have been extensively studied. Historically, much of the earlier work on CPA was motivated by its similarities in sequence and activity to the clinically important angiotensin-converting enzyme (ACE),[4] which plays an important role in the blood-pressure control mechanism, and its structure was not available until 2003.[5]

Numerous high-resolution structures of CPA have been determined in its apo form and in complexes with various substrates, substrate analogues, and transition-state analogues.[6−21] The binding of ligands has been observed to induce a large conformational change in Tyr248, resulting in a hydrogen bond between the phenolic hydroxyl group and the terminal carboxylate of the peptidyl substrate.[13] In addition, three CPA residues, namely Arg127, Asn144, and Arg145, also interact strongly with the same substrate carboxylate group as well as the carbonyl group in the peptide backbone. These interactions are believed to play an important role in both substrate binding and catalysis.

† Sichuan University.
‡ University of New Mexico.

(1) Vallee, B. L.; Galdes, A.; Auld, D. S.; Riordan, J. F. In *Zinc Enzymes*; Spiro, T. G., Ed.; Wiley: New York, 1983.
(2) Lipscomb, W. N. *Proc. Natl. Acad. Sci. U.S.A.* **1980**, *77*, 3875–3878.
(3) Christianson, D. W.; Lipscomb, W. N. *Acc. Chem. Res.* **1989**, *22*, 62–69.
(4) Ondetti, M. A.; Cushman, D. W. *Annu. Rev. Biochem.* **1982**, *51*, 283.
(5) Natesh, R.; Schwager, S. L. U.; Sturrock, E. D.; Acharya, K. R. *Nature* **2003**, *421*, 551–554.
(6) Rees, D. C.; Lipscomb, W. N. *J. Mol. Biol.* **1982**, *160*, 475–498.
(7) Rees, D. C.; Lipscomb, W. N. *Proc. Natl. Acad. Sci. U.S.A.* **1983**, *80*, 7151–7154.
(8) Rees, D. C.; Lipscomb, W. N. *J. Mol. Biol.* **1983**, *168*, 367–387.
(9) Christianson, D. W.; Lipscomb, W. N. *Proc. Natl. Acad. Sci. U.S.A.* **1985**, *82*, 6840–6844.
(10) Christianson, D. W.; Kuo, L. C.; Lipscomb, W. N. *J. Am. Chem. Soc.* **1985**, *107*, 8281–8283.
(11) Christianson, D. W.; Lipscomb, W. N. *J. Am. Chem. Soc.* **1986**, *108*, 545–546.
(12) Christianson, D. W.; Lipscomb, W. N. *J. Am. Chem. Soc.* **1986**, *108*, 4998–5003.
(13) Christianson, D. W.; Lipscomb, W. N. *Proc. Natl. Acad. Sci. U.S.A.* **1986**, *83*, 7568–7572.
(14) Christianson, D. W.; Lipscomb, W. N. *J. Am. Chem. Soc.* **1987**, *109*, 5536–5538.
(15) Christianson, D. W.; Lipscomb, W. N. *J. Am. Chem. Soc.* **1988**, *110*, 5560–5565.
(16) Kim, H.; Lipscomb, W. N. *Biochemistry* **1990**, *29*, 5546–5555.
(17) Mangani, S.; Carloni, P.; Orioli, P. *J. Mol. Biol.* **1992**, *223*, 573–578.
(18) Teplyakov, A.; Wilson, K. S. *Acta Crystallogr.* **1993**, *D49*, 534–540.
(19) Greenblatt, H. M.; Feinberg, H.; Tucker, P. A.; Shoham, G. *Acta Crystallogr.* **1998**, *D54*, 289–305.
(20) Cho, J. H.; Kim, D. H.; Chung, S. J.; Ha, N.-C.; Oh, B.-H.; Choi, K. Y. *Bioorg. Med. Chem.* **2002**, *10*, 2015–2022.
(21) Kilshtain-Vardi, A.; Glick, M.; Greenblatt, H. M.; Goldblum, A.; Shoham, G. *Acta Crystallogr.* **2003**, *D59*, 323–333.

10.1021/ja9027988 CCC: $40.75

Scheme 1. Two Putative Mechanisms for CPA Catalysis

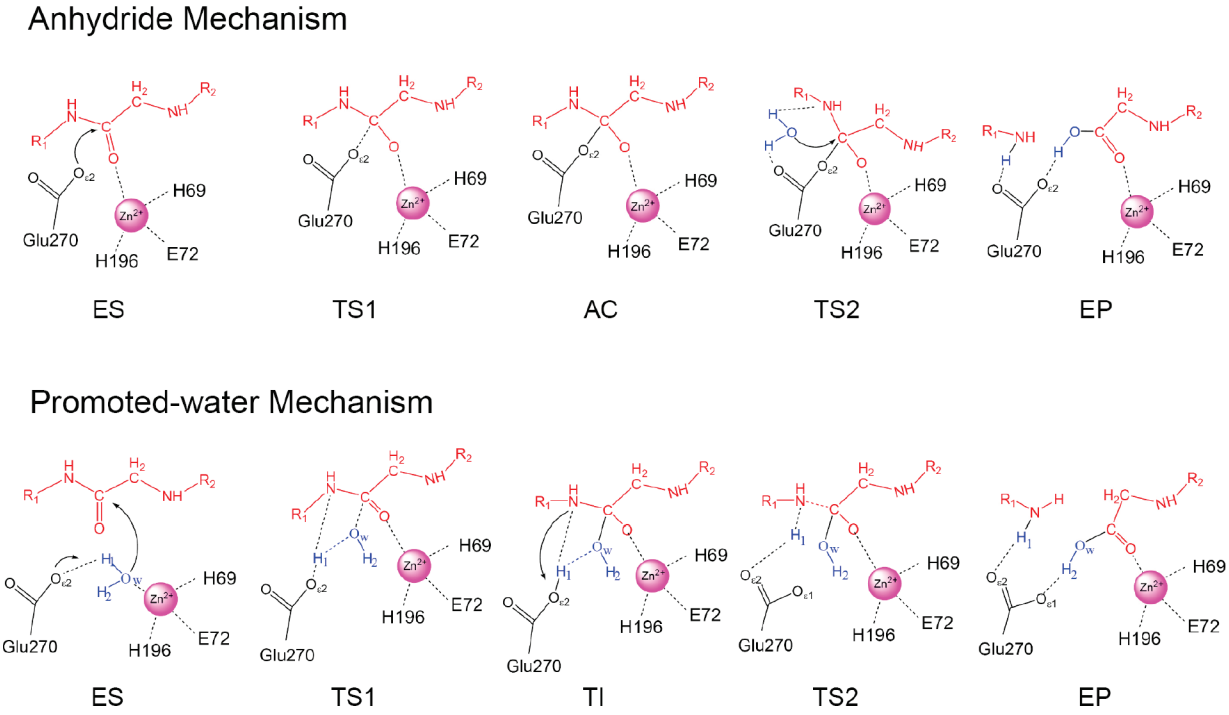

In particular, Arg127 is hydrogen-bonded with the scissile carbonyl oxygen, serving as the oxyanion hole to stabilize the tetrahedral intermediate.[15,22,23] Furthermore, the terminal side chain of the substrate is surrounded by a hydrophobic pocket in the so-called S_1' subsite, which is presumably responsible for the preference of CPA for aromatic terminal residues. In the catalytic S_1 subsite, the zinc cofactor is coordinated by three protein ligands, namely His196, Glu72, and His69, as well as a water molecule. A more recently determined high-resolution structure of CPA indicates that the zinc-bound water is most likely in its neutral state,[21] presumably due to its hydrogen bond with Glu270.

Despite extensive experimental studies, there is still no consensus on the catalytic mechanism of CPA.[2,3] Two major classes of mechanisms have been proposed, and they are depicted in Scheme 1. The *anhydride* mechanism envisages an acyl−enzyme intermediate resulting from direct nucleophilic attack of the scissile carbonyl carbon by the carboxylate side chain of Glu270, which is subsequently hydrolyzed by water to form the product. The alternative *promoted-water* mechanism stipulates instead a tetrahedral intermediate formed by nucleophilic attack of the zinc-bound water, activated by proton transfer to Glu270. The tetrahedral intermediate subsequently collapses upon protonation of the nitrogen leaving group by the Glu270 side chain. In a classical example of electrostatic catalysis,[24] Glu270 serves as a general base in the nucleophilic addition step and a general acid in the elimination step. Apparently, the roles played by the metal cofactor and by the key residue (Glu270) are quite different in the two mechanisms.

Experimental evidence supporting both mechanisms has been presented by several groups. In support of the promoted-water mechanism, Breslow and Wernick have shown in an ^{18}O isotope labeling experiment that the acyl−enzyme intermediate is unlikely to form in the hydrolysis of peptide substrates.[25,26] Later, cryospectrokinetic studies by Auld and co-workers[27,28] ruled out the existence of the acyl−enzyme intermediate in hydrolysis of both peptides and esters. However, there have also been reports of accumulating acyl−enzyme intermediates at low temperatures in ester hydrolysis catalyzed by CPA,[29−33] although some have questioned the correct identity of the intermediate.[34] It has been suggested that the hydrolysis mechanism might be different for ester and peptide substrates, because the former substrates typically bind with direct metal coordination by the scissile carbonyl, while such an interaction is considered nonproductive for the latter.[3] In 1998, Lee et al.[35] reported the detection of an anhydride intermediate in the CPA-catalyzed hydrolysis of glycyl-L-tyrosine by low-temperature solid-state NMR. However, it is worth noting that this substrate has a very slow hydrolysis rate.[36] In addition, the X-ray structure of the Michaelis complex indicates the absence of zinc-bound

(22) Phillips, M. A.; Fletterick, R.; Rutter, W. J. *J. Biol. Chem.* **1990**, *265*, 20692–20698.
(23) Phillips, M. A.; Rutter, W. J. *Protein Sci.* **1992**, *1*, 517–521.
(24) Jencks, W. P. *Catalysis in Chemistry and Enzymology*; Dover: New York, 1986.
(25) Breslow, R.; Wernick, D. L. *J. Am. Chem. Soc.* **1976**, *98*, 259–261.
(26) Breslow, R.; Wernick, D. L. *Proc. Natl. Acad. Sci. U.S.A.* **1977**, *74*, 1303–1307.
(27) Auld, D. S.; Galdes, A.; Geoghegan, K. F.; Holmquit, B.; Martinelli, R. A.; Vallee, B. L. *Proc. Natl. Acad. Sci. U.S.A.* **1984**, *81*, 5041–5045.
(28) Geoghegan, K. F.; Galdes, A.; Hanson, G.; Holmquit, B.; Auld, D. S.; Vallee, B. L. *Biochemistry* **1986**, *25*, 4669–4674.
(29) Makinen, M. W.; Kuo, L. C.; Dymowski, J. J.; Jaffer, S. *J. Biol. Chem.* **1979**, *254*, 356–366.
(30) Kuo, L. C.; Makinen, M. W. *J. Biol. Chem.* **1982**, *257*, 24–27.
(31) Suh, J.; Cho, W.; Chung, S. *J. Am. Chem. Soc.* **1985**, *107*, 4530–4535.
(32) Sander, M. E.; Witzel, H. *Biochem. Biophys. Res. Commun.* **1985**, *132*, 681.
(33) Britt, B. M.; Peticolas, W. L. *J. Am. Chem. Soc.* **1992**, *114*, 5295–5303.
(34) Hoffman, S. J.; Chu, S. S.-T.; Lee, H.-H.; Kaiser, E. T.; Carey, P. R. *J. Am. Chem. Soc.* **1983**, *105*, 6971–6973.
(35) Lee, H. C.; Ko, Y. H.; Baek, S. B.; Kim, D. H. *Bioorg. Med. Chem. Lett.* **1998**, *8*, 3379–3384.

water, apparently displaced by the substrate.[13] This controversy is still far from fully resolved.

Given the experimental difficulties in distinguishing the two mechanisms, it is desirable to address the mechanistic issues theoretically. Indeed, attempts have been made in the past in this direction. For instance, molecular dynamics (MD) simulations of CPA have been reported by Banci et al.,[37] who showed that the active-site structure does not exclude either mechanism. Quantum chemical investigations on biological zinc and its coordination can be traced back to the earlier work of Pullman[38] and of Allen.[39] For CPA catalysis, most quantum chemical studies have been performed with semiempirical methods.[40−44] These theoretical studies focused mostly on the promoted-water mechanism, but Vardi-Kilshtain et al.[44] have also presented some evidence against the anhydride mechanism. Although these pioneering studies provided valuable insights, they suffer from two major shortcomings. First, the validity of semiempirical models requires careful validation by higher-level theory, particularly when a transition metal is involved. Second, the quantum chemical studies did not take into consideration the protein environment, essential for catalysis. The enzymatic reaction is perhaps best modeled using a hybrid quantum mechanical and molecular mechanical (QM/MM) method,[45−49] in which the enzyme active site is treated quantum mechanically while the remainder of the protein is modeled with a MM force field. Indeed, such QM/MM studies have been reported for CPA, but only for its inhibition.[50,51]

In this publication, we examine the two mechanistic proposals using a hybrid QM/MM approach. In particular, the QM region is described by an approximate density functional approach, namely the self-consistent charge-density functional tight binding (SCC-DFTB) method,[52] while the MM region is described by the CHARMM force field. The SCC-DFTB Hamiltonian has been parametrized for biological zinc ions,[53] and the combined SCC-DFTB/CHARMM approach[54] has been shown to give a reasonably accurate description of several zinc enzymes.[55−61] In addition to the QM/MM studies, we also investigate the reaction pathways in truncated active-site models with high-level density functional theory (DFT) calculations in order to verify the validity of the conclusions reached by the QM/MM models.

2. Methods

2.1. QM/MM Models. The hybrid quantum mechanical and molecular mechanical approach[62] has been extensively applied to study enzymatic reaction mechanisms.[45−49] Such a method has the advantage that a very large system such as an enzyme can be investigated with manageable computation costs. The basic idea of the QM/MM scheme is to divide the system into two parts: the smaller QM region, where the chemical bond breaking and forming take place, while the surrounding region is described by a MM force field.

In the work reported here, we used the self-consistent charge-density functional tight binding (SCC-DFTB) model[52] to describe the QM region and the CHARMM all-atom force field[63] to characterize the MM region. The SCC-DFTB method is based on a second-order expansion of the total DFT energy with respect to the charge-density variation. It is much more efficient than ab initio QM/MM approaches and consequently amenable to free-energy calculations. The efficiency is essential for metallo-enzymes because the active site is often much too large for an accurate ab initio QM/MM free-energy simulation. The SCC-DFTB model has been extensively tested for enzyme systems,[48,54,64,65] including active sites with zinc cofactors.[53] The QM/MM approach based on the SCC-DFTB method has been shown to give a satisfactory description of several zinc enzymes, including carbonic anhydrase[55,56] and β-lactamases.[57−61]

The starting point of the simulation was selected from an enzyme−inhibitor complex structure (PDB code 6CPA), which is the wild-type (WT) bovine CPA complexed with the *O*-[[(1*R*)-[*N*-phenylmethoxycarbonyl)-L-alanyl]amino]ethyl]hydroxyphosphinyl]-L-3-phenyllactate ($ZAA^{p}(O)F$) inhibitor.[16] This structure was chosen because of the similarities between the inhibitor and a bona fide substrate of CPA, namely hippuryl-L-Phe (HPA, Scheme 2).[66] The HPA substrate was recovered manually by modifying the $ZAA^{p}(O)F$ inhibitor in the X-ray structure. A water molecule was added in the active site for studying the promoted-water pathway. Hydrogen atoms were added using the HBUILD utility in CHARMM, and the titratable residues in the enzymes were assigned the appropriate ionization states at pH = 7. In addition, the disulfide bond between Cys138 and Cys161 was enforced. All simulations were performed with the CHARMM suite of simulation codes.[67]

The resulting structure was then solvated by a pre-equilibrated sphere of TIP3P waters[68] with 25 Å radius centered at the zinc

(36) Quiocho, F. A.; Lipscomb, W. M. *Adv. Protein Chem.* **1971**, *25*, 1–78.
(37) Banci, L.; Bertini, I.; La Penna, G. *Proteins* **1994**, *18*, 186–197.
(38) Demoulin, D.; Pullman, A. *Theo. Chim. Acta* **1978**, *49*, 161.
(39) Kitchen, D. B.; Allen, L. C. *J. Phys. Chem.* **1989**, *93*, 7265.
(40) Alex, A.; Clark, T. *J. Comput. Chem.* **1992**, *13*, 704–717.
(41) Alvarez-Santos, S.; Gonzalez-Lafont, A.; Lluch, J. M. *Can. J. Chem.* **1994**, *72*, 2077.
(42) Alvarez-Santos, S.; Gonzalez-Lafont, A.; Lluch, J. M.; Oliva, B.; Aviles, F. X. *New J. Chem.* **1998**, 319–326.
(43) Kilshtain-Vardi, A.; Shoham, G.; Goldblum, A. *Int. J. Quantum Chem.* **2002**, *88*, 87–98.
(44) Vardi-Kilshtain, A.; Shoham, G.; Goldblum, A. *Mol. Phys.* **2003**, *101*, 2715–2724.
(45) Gao, J. In *Reviews in Computational Chemistry*; Lipkowitz, K. B., Boyd, D. B., Eds.; VCH: New York, 1996; Vol. 7, pp 119−185.
(46) Warshel, A. *Annu. Rev. Biophys. Biomol. Struct.* **2003**, *32*, 425–443.
(47) Zhang, Y. *Theor. Chem. Acc.* **2006**, *116*, 43–50.
(48) Riccardi, D.; Schaefer, P.; Yang, Y.; Yu, H.; Ghosh, N.; Prat-Resina, X.; Konig, P.; Li, G.; Xu, D.; Guo, H.; Elstener, M.; Cui, Q. *J. Phys. Chem. B* **2006**, *110*, 6458–6469.
(49) Hu, H.; Yang, W. *Annu. Rev. Phys. Chem.* **2008**, *59*, 573–601.
(50) Phoon, L.; Burton, N. A. *J. Mol. Graph. Model.* **2005**, *24*, 94–101.
(51) Cross, J. B.; Vreven, T.; Meroueh, S. O.; Mobashery, S.; Schlegel, H. B. *J. Phys. Chem. B* **2005**, *109*, 4761–4769.
(52) Elstner, M.; Porezag, D.; Jungnickel, G.; Elsner, J.; Haugk, M.; Frauenheim, T.; Suhai, S.; Seigert, G. *Phys. Rev.* **1998**, *B58*, 7260–7268.
(53) Elstner, M.; Cui, Q.; Munih, P.; Kaxiras, E.; Frauenheim, T.; Karplus, M. *J. Comput. Chem.* **2003**, *24*, 565–581.
(54) Cui, Q.; Elstner, M.; Kaxiras, E.; Frauenheim, T.; Karplus, M. *J. Phys. Chem. B* **2001**, *105*, 569–585.
(55) Riccardi, D.; Cui, Q. *J. Phys. Chem. A* **2007**, *111*, 5703–5711.
(56) Riccardi, D.; Konig, P.; Guo, H.; Cui, Q. *Biochemistry* **2008**, *47*, 2369–2378.
(57) Xu, D.; Zhou, Y.; Xie, D.; Guo, H. *J. Med. Chem.* **2005**, *48*, 6679–6689.
(58) Xu, D.; Xie, D.; Guo, H. *J. Biol. Chem.* **2006**, *281*, 8740–8747.
(59) Xu, D.; Guo, H.; Cui, Q. *J. Phys. Chem. A* **2007**, *111*, 5630–5636.
(60) Xu, D.; Guo, H.; Cui, Q. *J. Am. Chem. Soc.* **2007**, *129*, 10814.
(61) Wang, C.; Guo, H. *J. Phys. Chem. B* **2007**, *111*, 9986–9992.
(62) Warshel, A.; Levitt, M. *J. Mol. Biol.* **1976**, *103*, 227–249.
(63) MacKerell, A. D., Jr.; et al. *J. Phys. Chem. B* **1998**, *102*, 3586–3616.
(64) Sattelmeyer, K. W.; Tirado-Rives, J.; Jorgensen, W. L. *J. Phys. Chem. A* **2006**, *110*, 13551–13559.
(65) Otte, N.; Scholten, M.; Thiel, W. *J. Phys. Chem. A* **2007**, *111*, 5751–5755.
(66) Gardell, S. J.; Craik, C. S.; Hilvert, D.; Urdea, M. S.; Rutter, W. J. *Nature* **1985**, *317*, 551–555.
(67) Brooks, B. R.; Bruccoleri, R. E.; Olafson, B. D.; States, D. J.; Swaminathan, S.; Karplus, M. *J. Comput. Chem.* **1983**, *4*, 187–217.
(68) Jorgensen, W. L.; Chandrasekhar, J.; Madura, J. D.; Impey, R. W.; Klein, M. L. *J. Chem. Phys.* **1983**, *79*, 926–935.

Scheme 2. Atom Definition and Active-Site Interaction Pattern for the ES Complex of CPA

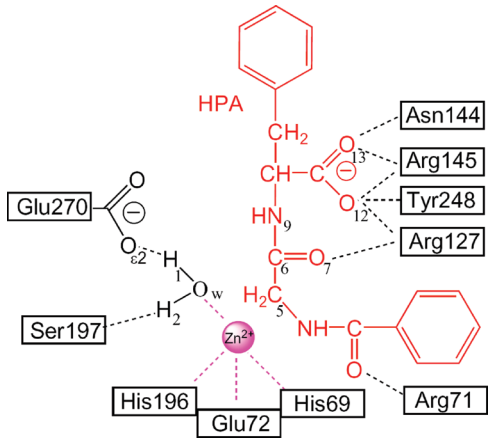

ion, followed by a 30 ps MD simulation with all protein and substrate atoms fixed. This process was repeated several times with randomly rotated water spheres to ensure uniform solvation. Subsequently, stochastic boundary conditions[69] were applied to the solvated enzyme system. In particular, atoms that are 25 Å away from the origin (Zn) were removed, while atoms in the buffer zone ($22 < r < 25$ Å) were subjected to Langevin dynamics with friction and random forces, as well as additional harmonic restraining forces. In the inner reaction zone ($r < 22$ Å), the atoms follow Newtonian dynamics on the hybrid QM/MM potential energy hypersurface. A group-based switching scheme was used for nonbonded interactions.[70]

The QM region includes the zinc ion, the side-chain atoms of its three protein ligands His69, Glu72, and His196, the zinc-bound water, the side-chain atoms of Arg127 and Glu270, and the entire substrate molecule. The QM boundaries were treated with the link atom approach,[71] in which a H atom is added to each C_β of the relevant amino acid. The QM region has a total of 125 atoms. In the R127A mutant calculations, the side chain of Arg127 is replaced by a methyl group for Ala. Furthermore, the water nucleophile was removed in studying the anhydride pathway.

To gain insight about the enzyme−substrate (ES) complex, we have carried out extensive MD simulations of the hybrid QM/MM system. The starting system was brought to room temperature (300 K) in 30 ps, followed by room temperature MD for another 70 ps to ensure the system is sufficiently equilibrated. The final 500 ps MD trajectory was used to for analysis. The integration step had a 1.0 fs time interval, and the SHAKE algorithm[72] was applied to maintain all covalent bonds-involved hydrogen atoms.

Several random snapshots were picked from the MD trajectory as the initial configurations for minimal energy path calculations. For the promoted-water pathway, two putative reaction coordinates are defined as follows. The reaction coordinate for the nucleophilic addition (NA) of the water nucleophile is given by the distance between the water oxygen (O_w) and the substrate carbonyl carbon (C_6): $r_1 = d_{O_w \cdots C_6}$. The corresponding reaction coordinate for the elimination (E) of the leaving group is given by the antisymmetric stretching coordinate of the proton (H_1) between $O_{\epsilon 2}$ of the general base (Glu270) and the substrate backbone amide nitrogen (N_9): $r_2 = d_{O_{\epsilon 2} \cdots H_1} - d_{N_9 \cdots H_1}$. For the anhydride pathway, the NA reaction coordinate is given by the distance between a Glu270 oxygen and the substrate carbonyl carbon: $r'_1 = d_{O_{\epsilon 2} \cdots C_6}$. The reaction paths were determined by adiabatic mapping along the putative reaction coordinates.

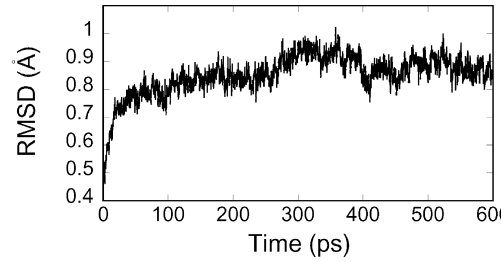

Figure 1. Rmsd for the QM/MM MD simulation of the ES complex of CPA.

To include the fluctuation and reorganization of the enzymatic system, we further computed potentials of mean force (PMFs) for the two mechanistic pathways. The minimum energy structures along a putative reaction coordinate were used as the initial points for the PMF calculations. The PMF calculations used umbrella sampling[73] with harmonic constraints of 100−200 kcal/mol·Å^2. For the NA and E steps of the promoted-water pathway, 12 and 9 windows were used, respectively. On the other hand, the anhydride PMF was obtained with 17 simulation windows.

In the PMF calculations, 60 ps equilibration simulations were first performed to bring the system to 300 K. The distribution function in the reaction coordinate was then collected in the subsequent 40 ps. The final PMF was obtained using the weighted histogram analysis method (WHAM).[74] During the PMF simulations, the SHAKE module was applied to all hydrogen atoms except hydrogen atoms on the zinc-bound water molecule.

2.2. DFT and Truncated Active-Site Models. Given the semiempirical nature of the SCC-DFTB Hamiltonian, it is important to provide an independent check of the results obtained by the QM/MM approach. In this work, we examined the reaction paths in several truncated active-site models using high-level DFT. The truncated active-site models consist of the zinc ion, the nucleophilic water for the promoted-water pathway, analogues of Glu270 and the three protein ligands of Zn(II), and the substrate analogue. In addition, we have included the side chains of Arg127 and Arg145 in our model to simulate the binding mode of C-terminal carboxylate group. For the substrate analogue, the phenol groups were removed to reduce computational costs. The total number of atoms is 98 for the promoted-water pathway and 74 for the anhydride pathway.

The B3LYP exchange-correlation functional[75,76] and a standard basis set of 6-31G(d) were used in fully geometrical optimization of stationary points, followed by harmonic vibrational frequencies calculations for confirmation. These stationary points were then connected by intrinsic reaction coordinate (IRC) method.[77] The solvent effects were studied with the PCM model[78] with dielectric constants of water ($\epsilon = 80$) and protein ($\epsilon = 5$). All of the computations were carried out using the Gaussian 03 suite of programs.[79]

3. Results

3.1. The Promoted-Water Pathway. 3.1.1. Enzyme−Substrate Complex. A 600 ps MD simulation was carried out for the ES complex using the hybrid QM/MM Hamiltonian. Figure 1 displays the root-mean-square deviation (rmsd) for the backbone atoms, which increases in the first 100 ps and then becomes relatively stable for the remaining 500 ps of simulation, with the

(69) Brooks, C. L., III; Karplus, M. *J. Mol. Biol.* **1989**, *208*, 159–181.
(70) Steinbach, P. J.; Brooks, B. R. *J. Comput. Chem.* **1994**, *15*, 667.
(71) Field, M. J.; Bash, P. A.; Karplus, M. *J. Comput. Chem.* **1990**, *11*, 700–733.
(72) Ryckaert, J. P.; Ciccotti, G.; Berendsen, H. J. *J. Comput. Phys.* **1977**, *23*, 327–341.
(73) Torrie, G. M.; Valleau, J. P. *J. Comput. Phys.* **1977**, *23*, 187–199.
(74) Kumar, S.; Bouzida, D.; Swendsen, R. H.; Kollman, P. A.; Rosenberg, J. M. *J. Comput. Chem.* **1992**, *13*, 1011–1021.
(75) Becke, A. D. *J. Chem. Phys.* **1993**, *98*, 5648–5652.
(76) Lee, C.; Yang, W.; Parr, R. G. *Phys. Rev. B* **1988**, *37*, 785–789.
(77) Gonzalez, C.; Schlegel, H. B. *J. Phys. Chem.* **1990**, *94*, 5523.
(78) Tomasi, J.; Persico, M. *Chem. Rev.* **1994**, *94*, 2027–2094.
(79) Frisch, M. J.; et al. *Gaussian 03*; Gaussian, Inc.: Pittsburgh, PA, 2003.

Table 1. Key Geometric Parameters of Stationary Points for the Promoted-Water Pathway Obtained at the B3LYP/6-31G(d) Level of Theory with the Truncated Active-Site Model and from QM/MM Simulations

	truncated model							
distance (Å)	ES	TS1	TI1	TI2	TS3	EP	QM/MM ES	QM/MM EP
$O_w \cdots C_6$	5.38	1.88	1.37	1.41	1.39	1.25	2.83 ± 0.22	1.32 ± 0.03
$H_1 \cdots O_{\epsilon 2}$(E270)	1.07	1.00	0.99	1.03	1.26	2.05	1.77 ± 0.14	
$H_2 \cdots O$(S197)							1.95 ± 0.23	
$Zn \cdots N_{\delta 1}$(H69)	2.01	2.12	2.04	2.06	2.05	2.02	1.99 ± 0.06	1.98 ± 0.06
$Zn \cdots O_{\epsilon 2}$(E72)	1.95	1.97	1.94	1.97	1.97	1.92	2.08 ± 0.07	2.05 ± 0.07
$Zn \cdots N_{\delta 1}$(H196)	2.05	2.07	2.03	2.05	2.04	2.03	1.97 ± 0.05	1.96 ± 0.05
$O_w \cdots Zn$	1.93	2.19	3.30	2.96	2.90	3.89	2.13 ± 0.08	3.44 ± 0.22
$Zn \cdots O_7$	5.51	2.06	1.94	1.94	1.95	1.95	4.19 ± 0.41	2.16 ± 0.09
$O_7 \cdots H_{21}$(R127)	1.83	1.89	1.67	1.88	1.89	2.97	2.37 ± 0.52	
$O_7 \cdots H_{11}$(R127)	3.00	2.91	3.00	3.71	3.71	5.24	2.64 ± 0.52	
$O_{12} \cdots H_{11}$(R127)	4.39	1.71	1.87	1.75	1.79	1.86	3.00 ± 0.48	
$O_{13} \cdots H_{22}$(N144)							1.85 ± 0.16	1.83 ± 0.15
$O_{12} \cdots H_{21}$(R145)	1.62	1.66	1.68	1.69	1.71	1.70	1.77 ± 0.18	1.73 ± 0.15
$O_{13} \cdots H_{11}$(R145)	1.70	1.66	1.63	1.67	1.69	1.69	1.95 ± 0.40	2.24 ± 0.63
$O_{12} \cdots H_H$(Y248)							1.67 ± 0.11	1.66 ± 0.11
$O_7 \cdots H_H$(Y248)							3.54 ± 0.34	
$C_5 \cdots C_6$	1.55	1.54	1.56	1.56	1.56	1.54		
$C_6 \cdots O_7$	1.24	1.30	1.37	1.37	1.36	1.28		
$C_6 \cdots N_9$	1.34	1.37	1.44	1.50	1.54	3.70		2.89 ± 0.38
$H_1 \cdots N_9$				1.72	1.26	1.03		
$O_1 \cdots H_{12}$(R71)							1.69 ± 0.11	1.73 ± 0.13
$O_1 \cdots H_{22}$(R127)							2.69 ± 0.58	2.03 ± 0.33

averaged rmsd of 0.87 ± 0.04 Å. The key internuclear distances averaged over the MD trajectory are listed in Table 1.

As shown by a snapshot of the ES complex in Figure 2, electrostatic interactions play an important role in substrate binding. In particular, the substrate C-terminal carboxylate group is anchored by strong hydrogen-bond interactions with the side-chain groups of Asn144, Arg145, Tyr248, and Arg127. In addition, Arg127 also forms a hydrogen bond with the scissile carbonyl oxygen (O_7). These hydrogen-bond interactions are consistent with known X-ray structures of CPA complexes.[15] No direct contact between the substrate and metal ion was found in our simulations, and the Zn−O_7 distance is 4.19 ± 0.41 Å. This observation suggests that the metal cofactor does not play a significant role in polarizing the substrate carbonyl group.

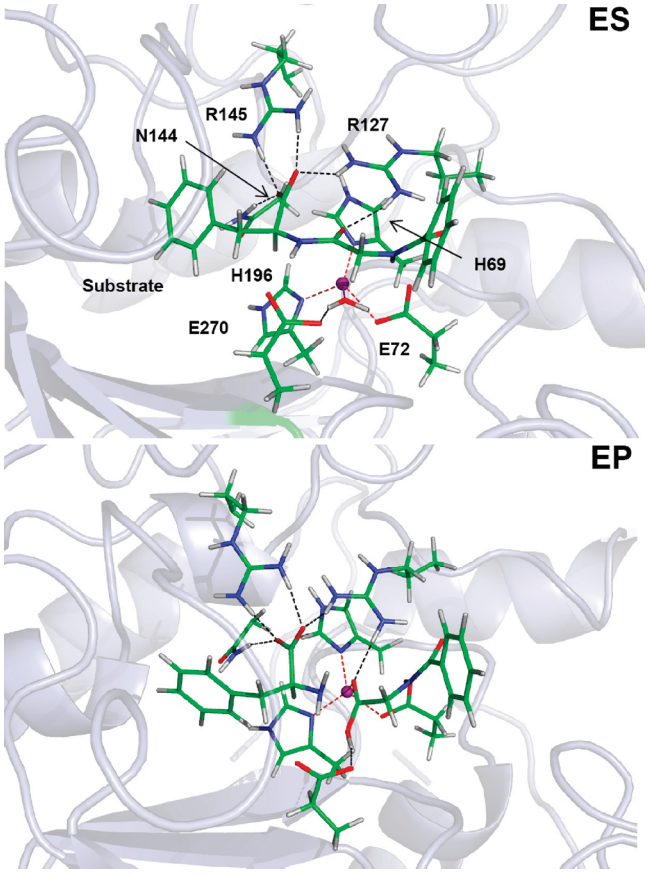

Figure 2. Snapshots of the ES and EP complexes in the promoted-water pathway, obtained from QM/MM simulations. Black dashed lines represent hydrogen bonds, while red dashed lines represent metal−ligand bonds.

The active-site water molecule is bound to Zn(II) as its fourth ligand with a distance of 2.13 ± 0.08 Å, which is slightly larger than the experimental value of 1.96 Å observed in a recent high-resolution X-ray structure.[21] The coordination of water with Zn(II) is consistent with its lowered pK_a (around 7) in CPA,[3] due to polarization by Zn(II).[38,39] The water molecule is also hydrogen-bonded with the side chain of Glu270 and the backbone oxygen of Ser197, in agreement with X-ray data.[8] The water nucleophile remains in a perfect near-attack position,with a distance to C_6 of 2.83 ± 0.22 Å. In addition, its strong hydrogen bond with the carboxylate of Glu270 ($r(O_{\epsilon 2}-H_1)$ = 1.77 ± 0.14 Å) sets the stage for the necessary proton transfer in the nucleophilic addition step. The interaction pattern of the ES complex is illustrated in Scheme 1.

3.1.2. PMF. The reaction via the promoted-water mechanism is initiated by the nucleophilic addition (NA) of the water nucleophile to the scissile carbonyl carbon (C_6), assisted by the general base Glu270. At the first transition state (TS1), the O_w-C_6 distance is 1.73 Å, and the central C_6 atom has distorted away from its planar geometry in ES. As shown in Figure 3, the proton transfer from the water nucleophile to Glu270 is concerted with NA, as evidenced by the partially formed bond between $O_{\epsilon 2}$ of Glu270 and the water proton (H_1) at TS1.

This NA step leads to a tetrahedral intermediate (TI) characterized by an sp^3 central carbon and a C_6-O_w distance of 1.52 Å. The resulting negative charge on the carbonyl oxygen (O_7) is stabilized by the zinc ion as it replaces the water as the fourth ligand of Zn(II). Hence, the metal cofactor serves as a Lewis acid in catalysis, and the formation of TI can be

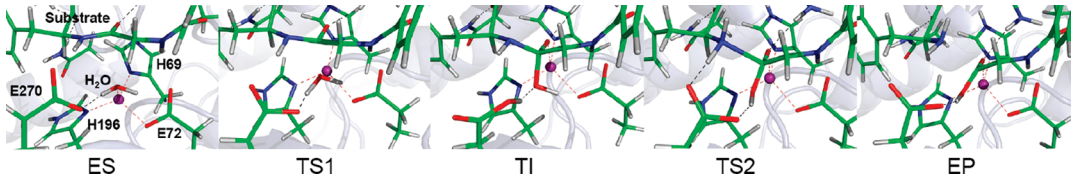

Figure 3. Active-site arrangements of the stationary points along the promoted-water reaction pathway obtained from QM/MM simulations.

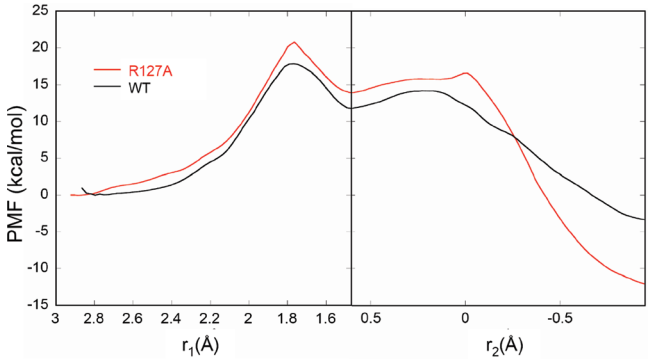

Figure 4. Potentials of mean force for the promoted-water pathway of the HPA hydrolysis catalyzed by the wild-type and R127A mutant of CPA.

considered as a ligand exchange reaction. In addition, O_7 is also hydrogen-bonded with the guanidinium group of Arg127, which serves with Zn(II) as the oxyanion hole in assisting the catalysis. The role of Arg127 in catalysis will be discussed further below. Interestingly, the protonated carboxylate of Glu270 flips and forms a hydrogen bond with the nitrogen atom (N_9) in the substrate, setting the stage for the second elimination step and its accompanying proton transfer. On the other hand, the other hydrogen of the nucleophile (H_2) maintains its hydrogen-bond interaction with the Ser197 backbone oxygen.

From the TI, the proton in the general acid (Glu270) is transferred from its $O_{\epsilon 2}$ site to the backbone amide nitrogen atom (N_9) of the substrate. As shown in Figure 3, the second transition state (TS2) is characterized by a N_9-C_6 distance of 2.05 Å. So the elimination (E) step is concerted with the proton-transfer process. At TS2, the $O_{\epsilon 1}$ atom of Glu270 is hydrogen-bonded with the H_2-O_w group, which breaks its hydrogen-bond interaction with Ser196.

During the entire reaction process, the coordination bonds between the zinc ion and its protein ligands are essentially unperturbed. So are the hydrogen-bond interactions between the substrate and the Asn144, Arg145, and Tys248 residues.

The promoted-water pathway described above is depicted in Figure 3 with active-site arrangements of the key stationary points. The corresponding PMF in Figure 4 indicates that this reaction has a typical nucleophilic substitution character, featuring a TI flanked by two transition states for the NA and E steps, respectively. The first NA step limits the rate with a barrier of 17.9 kcal/mol, while the second E step has a much smaller barrier of 2.4 kcal/mol. These data are in fairly good agreement with the experimental activation free energy of 15.7 kcal/mol for the catalyzed reaction estimated from $k_{cat} = 17.7 \pm 0.7\ s^{-1}$,[66] using transition-state theory with the assumption of a unit transmission coefficient.

As discussed above, Arg127 appears to play an important role in catalysis. In addition to its role in substrate binding, it serves, along with the zinc ion, as the oxyanion hole. Experimental studies have found that Arg127 mutations led to significant reduction of the catalytic activity of CPA,[22] and the activity of the mutants can be rescued by guanidine derivatives.[23] To achieve a more quantitative understanding of its role in catalysis, we have carried out PMF calculations for the R127A mutant using essentially the same protocol used in the WT calculations. The replacement of the guanidinium group by a methyl group forfeits the possibility of hydrogen bonding for the carbonyl oxygen (O_7), thus reducing the efficiency of the catalytic machinery. Figure 4 shows that the PMF for the R127A mutant has a higher barrier than that of the WT by about 3.0 kcal/mol. This is in reasonable agreement with the experimental $\Delta\Delta G = 3.4-6.0$ kcal/mol, depending on the substrate.[22] Except for the higher barrier, the reaction mechanism of the mutant remains the same.

3.1.3. Enzyme−Product Complex. As shown in Figure 2, the enzyme−product (EP) complex features a cleaved amide bond between the benzoyl-Gly carboxylate carbon (C_6) and the backbone amide nitrogen (N_9) of Phe in the substrate. We have carried out a 600 ps MD study of the EP complex within the same QM/MM framework, and the results are listed in Table 1. The C_6-N_9 distance is about 2.89 ± 0.38 Å in the EP complex. The newly formed carboxylate oxygen (O_7) replaces the water as the fourth ligand of the zinc cofactor, while the other three ligand−metal bonds are largely unchanged. The carboxylate group of Phe is hydrogen-bonded with Asn144, Arg145, and Tyr248. Arg127 moves away from the Gly carboxylate and forms a strong hydrogen bond to the benzoyl carbonyl oxygen, to help in positioning the benzoyl-Gly species. The carboxylate of Glu270 is now engaged in hydrogen bonding with both the amide group and the carboxylate group of the two products. On the other hand, Tyr248 maintains the hydrogen bond with one of the oxygen atoms of the C-terminal carboxylate group, but it does not seem to participate in the reaction in any significant way, an observation consistent with experimental data.[66,80] The major function of Tyr248 appears to assist the substrate binding. However, these data do not exclude the possibility that Tyr248 plays some role in CPA catalysis.[81]

3.1.4. Truncated Active-Site Model. The DFT investigations of the truncated active-site model at the B3LYP/6-31G(d) level identified six stationary points along the reaction path. The geometries and energies of these stationary points are listed in Tables 1 and 2, respectively. From Table 2, it can be seen that the inclusion of diffuse functions and polarization functions in the basis set did not qualitatively change the picture of the reaction path. Solvation effects are quite significant, which implies an important role of the local solvation environment in the enzyme. Finally, the SCC-DFTB method yields results qualitatively similar to those obtained with DFT, which provides further support for the validity of our QM/MM model.

The geometry of the ES complex in the truncated active-site model is very similar to that seen in our QM/MM simulations, featuring a tetra-coordinated Zn(II) and an intact peptide amide C_6-N_9 bond in the substrate. The zinc-bound water shares one of its protons with the carboxylate group of Glu270. The product EP complex, on the other hand, has a cleaved peptide amide bond. In addition, the water ligand of the Zn(II) cofactor is

Table 2. Energetics of the Truncated Active-Site Model for the Promoted-Water Pathway at the B3LYP/6-31G(d) Level of Theory (Energy in kcal/mol)

methods	ES	TS1	TI1	TI2	TS3	EP
energy (B3LYP/6-31G(d))	0.0	41.49	33.35	14.92	17.56	−4.81
free energy (B3LYP/6-31G(d))	0.0	42.28	34.83	18.35	19.55	−5.06
PCM (B3LYP/6-31G(d) w/ϵ=80)	0.0	26.92	20.23	3.40	2.91	−10.34
PCM (B3LYP/6-31G(d) w/ϵ=5)	0.0	33.32	25.21	9.00	9.99	−8.92
energy (B3LYP/6-31+G(d,p)//B3LYP/6-31G(d))	0.0	43.13	34.50	17.41	19.88	−0.72
energy (SCC-DFTB//B3LYP/6-31G(d))	0.0	31.56	21.29	5.79	8.23	−10.36

replaced in EP by the substrate carbonyl oxygen (O_7), while the Glu270 carboxylate forms hydrogen bonds with the newly formed amide and the carboxylate group in the products.

As shown in Figure 5, the rate-limiting transition state (TS1) features the NA of the water nucleophile to the scissile carbonyl carbon (C_6), which leads to a tetrahedral intermediate (TI1). The other transition state (TS3) is dominated by the proton transfer from the general base (protonated Glu270) and the nitrogen leaving group (N_9), leading to the cleavage of the amide C_6-N_9 bond. Interestingly, the tetrahedral intermediate (TI2) correlating with TS3 is somewhat different from TI1, due to a conformational change of the Glu270 carboxylate, which allows the formation of a hydrogen bond between the Glu270 proton and the backbone nitrogen (N_9). The energy of TI2 is lower than that of TI1 by 16.5 kcal/mol, due to an additional hydrogen bond between $O_{\epsilon 1}$ of Glu270 and the H_2 atom of the nucleophilic hydroxide. However, this large difference might be artificial because our truncated active-site model did not include the backbone carbonyl oxygen of Ser197, which was shown in the QM/MM simulation to form a hydrogen bond with the water nucleophile. Unfortunately, the transition state between TI1 and TI2 was not found despite many attempts, but there is little reason to believe that this illusive transition state is rate-limiting. The structures of all stationary points are given in the Supporting Information.

Despite some minor differences, the overall reaction pathway in the truncated active-site model mapped out with DFT is similar to that obtained in our QM/MM simulations. The overall reaction is dominated by the NA step, leading to a TI. The second elimination step is initiated by the proton transfer from the general base (Glu270) to the backbone amide nitrogen, which eventually leads to the cleavage of the amide C_6-N_9 bond. Like in the QM/MM simulations, the second step has a relatively low barrier. In addition, there are strong hydrogen bonds between Arg127 and Arg145 and the oxygen atoms in the substrate throughout the reaction. In particular, the carbonyl oxygen (O_7) is hydrogen-bonded with Arg127, which serves along with Zn(II) as the oxyanion hole.

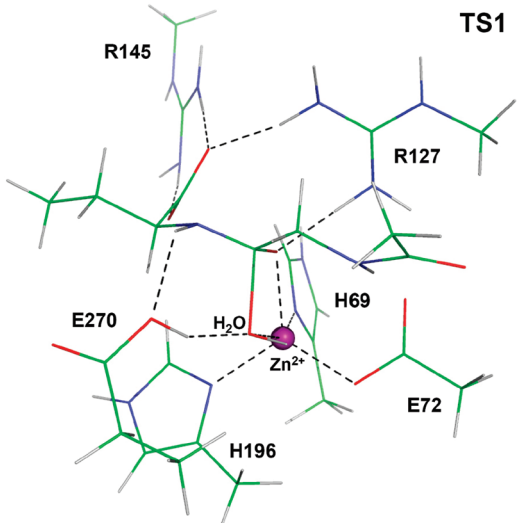

Figure 5. Structure of the rate-limiting transition state (TS1) for the truncated active-site model of the promoted-water pathway obtained at the B3LYP/6-31G(d) level of theory.

Our DFT results are similar to the results of an earlier AM1 study of the same reaction by Alvarez-Santos et al.,[41] who also used a truncated active-site model which is smaller than ours reported here. In their work, four transition states were found, and the reaction is limited by the NA of the water nucleophile and the proton transfer from Glu270 carboxylate to the amide nitrogen, which have energies of 37.90 and 39.97 kcal/mol, respectively. Small barriers have also been found for the initial deprotonation of the water nucleophile by Glu270 and for the final cleavage of the C−N bond. On the other hand, our results bear little resemblance with the other semiempirical study by Kilshtain-Vardi et al.,[43] who used the MNDO/d/H model.

3.2. Anhydride Pathway. 3.2.1. ES Complex. We have also explored the anhydride pathway using the same QM/MM approach. Because of the absence of the water nucleophile in this mechanism, the carbonyl oxygen (O_7) of the substrate is now in direct contact with the metal cofactor, serving as its fourth ligand. This is consistent with structural data in the literature when the water ligand is displaced.[3] Following essentially the same setup protocol, a 300 ps MD simulation was then carried out to test the stability of the ES complex, and a snapshot is displayed in Figure 6. Throughout the dynamics simulation, the substrate carbonyl oxygen (O_7) forms a very stable bond to the Zn ion. The $O_{\epsilon 2}$ atom of Glu270 was found to locate about 3.5 Å away from the HPA peptide carbonyl carbon (C_6), forming a near-attack position for the anhydride mechanism. However, as discussed below, the nucleophile is poorly aligned for the nucleophilic attack.

3.2.2. PMF. The corresponding PMF along the putative NA reaction coordinate ($r'_1 = d_{O_{\epsilon 2}-C_6}$) was obtained using essentially the same protocol as described above. As $O_{\epsilon 2}$ approaches C_6, the latter becomes increasingly pyramidal as it makes the transition from sp^2 to sp^3 hybridization. In the mean time, the carbonyl oxygen (O_7) approaches Zn(II) as its fractional negative charge builds up. As shown in Figure 7, however, the free energy increases as the Glu270 nucleophile attacks C_6 of the substrate. Apart from the shallow minimum near $r'_1 = 2.1$ Å, the PMF is essentially a monotonically increasing function of the reaction coordinate. The minimum is unlikely the acyl−enzyme intermediate, because the $O_{\epsilon 2}-C_6$ distance is too large to be covalent. It is probably due to some local conformational

(80) Hilvert, D.; Gardell, S. J.; Rutter, W. J.; Kaiser, E. T. *J. Am. Chem. Soc.* **1986**, *108*, 5298–5304.
(81) Cho, J. H.; Kim, D. H.; Kim, D.-H.; Lee, K. J.; Choi, K. Y. *Biochemistry* **2001**, *40*, 10197–10203.

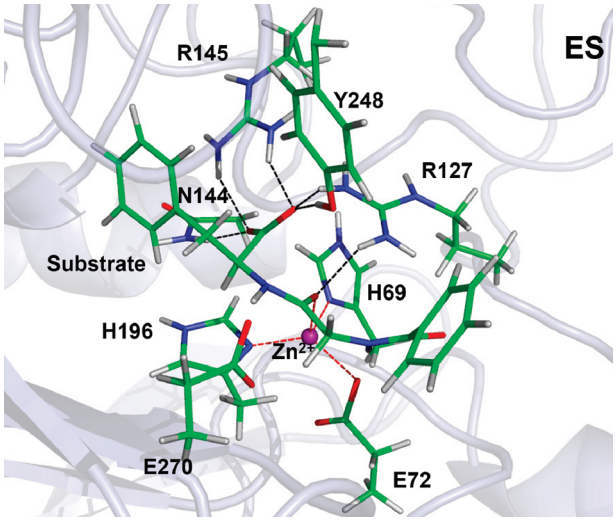

Figure 6. Snapshot of the QM/MM ES complex for the anhydride reaction pathway. Black dashed lines represent hydrogen bonds, while red dashed lines represent metal−ligand bonds.

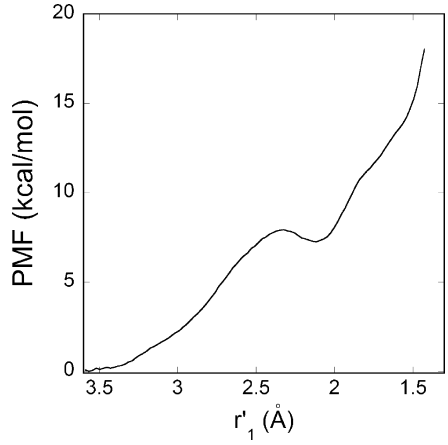

Figure 7. Potential of mean force for the anhydride pathway of the HPA hydrolysis.

minimum in the active site. The absence of a PMF minimum corresponding to the acyl−enzyme intermediate indicates that the anhydride pathway is not viable, at least for the HPA substrate.

3.2.3. Truncated Active-Site Model. To confirm the QM/MM results for the anhydride pathway, we have carried out high-level DFT (B3LYP/6-31G(d)) studies with a truncated active-site model, which is similar to that used for the promoted-water case. All attempts to locate the transition state for the NA step and the acyl−enzyme intermediate failed. Figure 8 displays the minimal energy path along the $O_{\epsilon 2}-C_6$ reaction coordinate, and it clearly shows a monotonic increase of energy without a barrier, consistent with the QM/MM PMF. The structures of the ES minimum and the high-energy complex corresponding to the $O_{\epsilon 2}-C_6$ distance of 1.47 Å were also included in the figure. The sp^2 and sp^3 geometries of C_6 in the two structures are apparent.

4. Discussion

CPA bears many similarities to thermolysin, which is also a peptidase with a zinc cofactor. Unlike CPA, thermolysin is an endopeptidase that cleaves peptide bonds containing hydrophobic residues.[82] In thermolysin, the zinc ion is also coordinated by two His residues and a Glu residue, as well as a water molecule. However, the two enzymes differ in many other aspects, including their structures. As in the CPA case, the catalytic mechanism of thermolysin was also uncertain.[82] The favored mechanism involves Glu143, which serves as a general base to activate the zinc-bound water. The NA of the hydroxide group to the substrate carbonyl carbon results in a tetrahedral intermediate, which eventually collapses to form the products. In the E step, a proton is transferred from the Glu143 general acid to the nitrogen leaving group in the substrate. This mechanism is essentially the same as the promoted-water pathways discussed here for CPA.

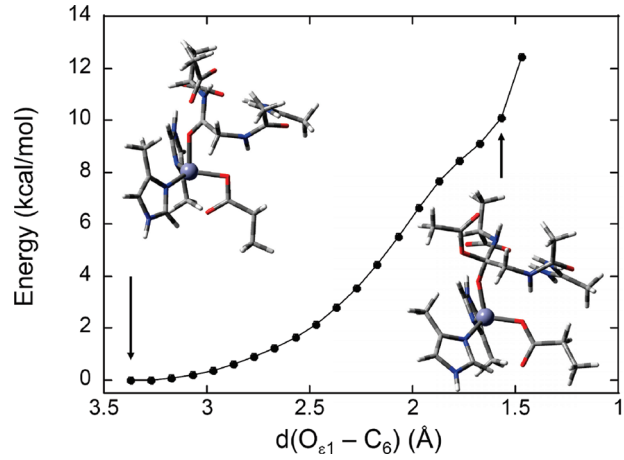

Figure 8. Energy profile of a truncated active-site model for the anhydride pathway at the B3LYP/6-31G(d) level of theory. The structure of the ES complex and that corresponding to the TI complex are shown as well.

In a recent ab initio QM/MM free-energy simulation, Blumberger et al. have convincingly demonstrated that the general base−general acid mechanism is indeed the preferred mechanism for thermolysin.[83] These authors found that the PMF has two transition states, with the first barrier for NA slightly higher than the second one for the E step. The overall free-energy barrier height is 14.8 kcal/mol, very close to what we have found for CPA. The zinc cofactor was also found to stabilize the negatively charged carbonyl oxygen of the scissile peptide bond, although it has weak interactions with the substrate in the ES complex. Since CPA and thermolysin have similar active-site arrangements, it is not surprising that they have the same catalytic mechanism.

The lack of direct interaction between Zn(II) and the scissile carbonyl in the ES complex is an important feature shared by thermolysin and CPA. Christianson and Lipscomb argued that a direct metal−carbonyl interaction found in several CPA−inhibitor complexes represents a nonproductive binding mode for CPA, because the zinc ion in such an configuration could not activate the water nucleophile.[3] Our simulation results concerning this key interaction, along with the work of Blumberger et al. on thermolysin,[83] provided strong evidence in support of this argument. It can thus be concluded that the metal cofactor in zinc hydrolases does not play a role in polarizing the substrate carbonyl. Rather, it serves as a Lewis acid to activate the water nucleophile and to stabilize the transition state. The similarities between the two quite different enzymes underscore convergent evolution of the two catalysts.

(82) Lipscomb, W. M.; Strater, N. *Chem. Rev.* **1996**, *96*, 2375–2433.
(83) Blumberger, J.; Lamoureux, G.; Klein, M. L. *J. Chem. Theor. Comput.* **2007**, *3*, 1837–1850.

The general base−general acid mechanism for both CPA and thermolysin has also been implicated in several other monozinc hydrolases. For example, members of the B2 subclass of β-lactamases such as CphA,[84] which has one Zn(II) cofactor, catalyze the breaking of the amide bond in β-lactam antibiotics using an active-site water promoted by a zinc-bound Asp residue.[58] It was also found recently in a DFT QM/MM study[85] that class I and II histone deacetylases, another type of monozinc hydrolases, use an active-site His residue to promote a water nucleophile in a general base−general acid mechanism.

Although uncommon in enzymatic systems, a carboxylate nucleophile is not without precedent. For example, a Meisenheimer complex is known to exist in the catalysis of dechlorination of 4-chlorobenzoyl-CoA by 4-chlorobenzoyl-CoA dehalogenase, in which an Asp residue serves as the nucleophile.[86,87] An anhydride intermediate has also been found in the hydrolysis of a thioester (3-hydroxyisobutyryl-CoA) to 3-hydroxyisobutyrate catalyzed by 3-hydroxyisobutyryl-CoA hydrolase.[88] To our best knowledge, however, there has been essentially no clear-cut evidence for an anhydride intermediate in amide hydrolysis. Our results, from both QM/MM and DFT calculations, clearly discount the anhydride mechanism, at least for the HPA substrate. It is somewhat surprising that no acyl−enzyme intermediate can be found for the anhydride pathway in both the QM/MM and DFT calculations, given the fact that the zinc ion provides significant stabilization of the oxyanion. The inability to form an acyl−enzyme intermediate is presumably due to a number of factors. First, the carboxylate group is a rather poor nucleophile, with a Swain−Scott value of 2.72.[24] Its nucleophilicity is further eroded by the hydrogen bond formed between $O_{\epsilon 1}$ and the NH moiety in the substrate backbone. [Interestingly, an acyl−enzyme intermediate has been observed to form in our DFT calculations when the amide is replaced by an ester, which has no hydrogen bond with the nucleophile (see Supporting Information). The preference of ester substrates in the anhydride mechanism has been extensively discussed before,[3] and we plan to investigate this possibility in more detail in the future.] Second, the conjugation between the carbonyl group and the adjacent amide group reduces the electrophilicity of the carbonyl carbon. Finally, the Glu270 carboxylate is not well aligned in the ES complex for NA of the substrate carbonyl carbon. The $O_{\epsilon 2}-C_6-O_7$, $O_{\epsilon 2}-C_6-N_9$, and $O_{\epsilon 2}-C_6-C_7$ angles are 140°, 79°, and 54°, respectively, far from the ideal value of 90°. The misalignment results in substantial stress in the system when the Glu270 carboxylate attacks the scissile carbonyl carbon. These factors make the formation of the acyl−enzyme intermediate very unfavorable.

5. Conclusions

Despite the fact that CPA is one of the most extensively studied zinc enzymes, its catalytic mechanism has not been completely settled. In this work, we reported the first hybrid QM/MM and DFT studies on the hydrolysis reaction catalyzed by CPA using HPA as the substrate molecule. Both QM/MM simulations and DFT calculations support the hypothesis that the CPA-catalyzed hydrolysis reaction for peptide substrates is through the promoted-water pathway. In particular, Glu270 serves as the general base to facilitate the nucleophilic attack of the substrate carbonyl carbon by the deprotonated water nucleophile. Subsequently, the protonated carboxylate group of Glu270 acts as a general acid by donating the proton to the amide nitrogen leaving group, leading to the cleavage of the peptide C−N bond in the substrate. Free-energy calculations indicated that the first nucleophilic addition is the rate-limiting step, with a barrier of 17.9 kcal/mol, in reasonable agreement with experimental data. On the other hand, the free-energy well of the tetrahedral intermediate is relatively shallow toward the cleavage of the peptide CN bond.

The catalysis is assisted by the zinc cofactor, which serves as the Lewis acid. Its role is twofold. First, it activates the water nucleophile bound to Zn(II), and second, along with Arg127, it stabilizes the fractionally charged carbonyl oxygen of the substrate in the tetrahedral intermediate. The first role has been recognized since the work of Demoulin and Pullman,[38] and there are numerous examples of Zn(II) serving as an oxyanion hole in enzyme catalysis.[82] However, our calculations indicate that the zinc ion in CPA does not play a significant role in polarizing the substrate carbonyl. Rather, the polarization is largely due to Arg127, which is hydrogen-bonded with the carbonyl oxygen of the substrate. Free-energy simulations concluded that the contribution of this residue leads to about 3 kcal/mol reduction of the rate-limiting barrier, in agreement with experiment.

Our results also provided strong evidence against the anhydride mechanism in CPA catalysis, at least for the HPA substrate. The free-energy profile suggested that no acyl−enzyme intermediate can be formed. However, preliminary results indicate that such a mechanism is possible for ester substrates.

Acknowledgment. This work was supported by the National Natural Science Foundation of China (No. 20803048 to D.X.) and by the National Institutes of Health (R03-AI068672 and R03-AI071992 to H.G.). Some of the calculations have been performed at the National Centers for Supercomputing Applications. We also acknowledge Q. Cui for helping with the SCC-DFTB simulations and D. Dunaway-Mariano for some stimulating discussions.

Supporting Information Available: DFT stationary point structures along the promoted-water pathway for the peptide substrate and those for the anhydride pathway for the ester substrate; complete refs 63 and 79. This material is available free of charge via the Internet at http://pubs.acs.org.

JA9027988

(84) Garau, G.; Bebrone, C.; Anne, C.; Galleni, M.; Frere, J.-M.; Dideberg, O. *J. Mol. Biol.* **2005**, *345*, 785–795.
(85) Corminboeuf, C.; Hu, P.; Tuckerman, M. E.; Zhang, Y. *J. Am. Chem. Soc.* **2006**, *128*, 4530–4531.
(86) Yang, G.; Liu, R.-Q.; Taylor, K. L.; Xiang, H.; Price, J.; Dunaway-Mariano, D. *Biochemistry* **1996**, *35*, 10879–10885.
(87) Xu, D.; Wei, Y.; Wu, J.; Dunaway-Mariano, D.; Guo, H.; Cui, Q.; Gao, J. *J. Am. Chem. Soc.* **2004**, *126*, 13649–13658.
(88) Wong, B. J.; Gerlt, J. A. *J. Am. Chem. Soc.* **2003**, *125*, 12076–12077.